*International Journal of Thermophysics, Vol. 17, No. 2, 1996*

# Thermal Conductivity and Viscosity of 2,2-Dichloro-1,1,1-Trifluoroethane (HCFC-123)

**Y. Tanaka[1,2] and T. Sotani[1]**

*Received May 30, 1995*

The thermal conductivity and the viscosity data of CFC alternative refrigerant HCFC-123 (2,2-dichloro-1,1,1-trifluoroethane; $CHCl_2$-$CF_3$) were critically evaluated and correlated on the basis of a comprehensive literature survey. Using the residual transport-property concept, we have developed the three-dimensional surfaces of the thermal conductivity–temperature–density and the viscosity–temperature–density. A dilute-gas function and an excess function of simple form were established for each property. The critical enhancement contribution was taken no account because reliable crossover equations of state and the thermal conductivity data are still missing in the critical region. The correlation for the thermal conductivity is valid at temperatures from 253 to 373 K, pressures up to 30 MPa, and densities up to 1623 $kg \cdot m^{-3}$. The correlation for the viscosity is valid at temperatures from 253 to 423 K, pressures up to 20 MPa, and densities up to 1608 $kg \cdot m^{-3}$. The uncertainties of the present correlations are estimated to be 5% for both properties, since the experimental data are still scarce and somewhat contradictory in the vapor phase at present.

**KEY WORDS:** 2,2-dichloro-1,1,1-trifluoroethane; HCFC-123; R123; thermal conductivity; thermal diffusivity; transport properties; viscosity.

## 1. INTRODUCTION

Several years have already passed since a program was started to develop new environmentally acceptable CFC alternative refrigerants and to investigate their thermophysical properties all over the world. HCFC-123 (2,2-dichloro-1,1,1-trifluoroethane) has been considered a promising substitute for CFC-11 (trichlorofluoromethane), one of the most widely used

[1] Department of Chemical Science and Engineering, Faculty of Engineering, Kobe University, Rokkodai-cho, Nada-ku, Kobe 657, Japan.
[2] To whom correspondence should be addressed.



840/17/2-2

CFC refrigerants. In recent years, however, the selection criteria of alternative refrigerants have become more and more difficult from the view points of both the environmental properties of refrigerants such as ozone-depleting potential and global-warming potential and the cycle-performance characteristics such as energy efficiency and refrigerating capacity. CFCs and, now, HCFCs regulations have been accelerated in association with recent findings of ozone depletion. Concerns in the last several years have changed the situation in research and development of the alternative refrigerants considerably. The investigation of the thermophysical properties of alternative refrigerants is now concentrated mainly on HFCs and their mixtures as well as natural refrigerants to search for so-called a "post HCFC-22."

In spite of the rapid transition of our concern to new, more environmentally friendly working fluids, there is a definite need for good data and models of the thermophysical properties of more or less new alternative refrigerants and their mixtures. Two annexes of the International Energy Agency (IEA) Program on Advanced Heat Pumps [1] have dealt with such works, namely, Annex XIII-State and Transport Properties of High Temperature Working Fluids and Nonazeotropic Mixtures and Annex XVIII-Thermophysical Properties of the Environmentally Acceptable Refrigerants. At the fifth meeting of Annex XVIII held in Maastricht, The Netherlands, on April 30, 1993, the equation of state developed by Tillner-Roth and Baehr [2] for HFC-134a and that of Younglove and McLinden [3] for HCFC-123 have been authorized internationally as the standard equations of state. Concerning the transport properties, new correlations of HFC-134a have been presented by Krauss et al. [4]. This paper is a continuation of our group work under the auspices of IEA on the transport properties of alternative refrigerants. In the present work, the thermal conductivity and the viscosity data of HCFC-123, which has been investigated most often among the alternative refrigerants together with HFC-134a, were critically evaluated and correlated on the basis of a comprehensive literature survey.

## 2. THERMODYNAMIC KEY DATA

The critical evaluation and correlation of the transport properties require the knowledge of basic thermodynamic data such as the critical parameters, a vapor-pressure equation, and a thermal equation of state to convert the temperature and pressure coordinates of the transport properties into those of the temperature and density. For this purpose we adopted the equation of state developed by Younglove and McLinden [3]. The critical parameters cited are (see Appendix I)

$$T_c = 456.831 \text{ K}, \qquad P_c = 3.668 \text{ MPa}, \qquad \rho_c = 550 \text{ kg} \cdot \text{m}^{-3}$$

The vapor-pressure equation presented by Japanese Association of Refrigeration [5] was also used to calculate the vapor pressure conveniently.

$$\ln(P_r) = T_r^{-1}[-7.5998(1-T_r) + 3.0970(1-T_r)^{1.5} - 3.014(1-T_r)^2 - 0.864(1-T_r)^3] \quad (1)$$

where $P_r = P/3.666$ MPa, and $T_r = T/456.86$ K.

## 3. CORRELATION PROCEDURE

According to the residual transport property concept [6–11], the thermal conductivity $\lambda(\rho, T)$ of a pure fluid at a given density $\rho$ and temperature $T$ can be considered to be composed of three terms as follows:

$$\lambda(\rho, T) = \lambda_0(T) + \Delta\lambda_R(\rho, T) + \Delta\lambda_c(\rho, T) \quad (2)$$

where $\lambda_0(T)$ is a dilute-gas term ($\lambda$ at the zero density limit) which depends on temperature only, $\Delta\lambda_R(\rho, T)$ is an excess term (residual term) which accounts for the density or pressure dependence, respectively, and $\Delta\lambda_c(\rho, T)$ is a contribution which represents the critical enhancement in a region extending around the critical point. However, it is generally found for pure simple fluids that the representation of the excess term $\Delta\lambda_R(\rho, T)$ as a function of density and temperature does not show any significant temperature dependence within the uncertainty of the measurements up to three times the critical density. Therefore, Eq. (2) is simplified as

$$\lambda(\rho, T) = \lambda_0(T) + \Delta\lambda_R(\rho) + \Delta\lambda_c(\rho, T) \quad (3)$$

This equation can be used to correlate and calculate the three-dimensional surfaces of the thermal conductivity as a function of temperature and density.

The correlation of the viscosity can be also carried out according to the residual viscosity concept which asserts that the viscosity $\eta(\rho, T)$ at a given density and temperature can be split into a dilute-gas term $\eta_0(T)$ which depends on temperature only, and into an excess term $\Delta\eta_R(\rho, T)$. Strictly speaking, the third contribution, $\Delta\eta_c(\rho, T)$, the critical enhancement of the viscosity should be added around the critical point. However, it is quite small for the viscosity and can be neglected in a practical correlation [7, 9]. Hence,

$$\eta(\rho, T) = \eta_0(T) + \Delta\eta_R(\rho, T) \quad (4)$$

Concerning the viscosity of polar refrigerants, however, the initial density coefficient of the viscosity, $(\partial\eta/\partial\rho)_T$ in the vapor phase definitely depends

on temperature. At low temperatures, $(\partial\eta/\partial\rho)_T$ is negative. It increases with increasing temperature gradually and becomes positive at high temperatures going through zero at a specific inversion temperature. Therefore, the temperature dependence in $\Delta\eta_R(\rho, T)$ cannot be neglected for the viscosity. Hence, either Eq. (4) or the following equation may be used for the viscosity correlation:

$$\eta(\rho, T) = \eta_0(T) + \eta_1(T)\rho + \Delta\eta_R(\rho) \tag{5}$$

where $\eta_1(T)\rho$ is an initial density dependence term which represents the density dependence of the viscosity at low densities, and $\Delta\eta_R(\rho)$ is an excess term which accounts for the density dependence at higher densities where a dependence on temperature can be neglected.

## 4. DATA SURVEY AND CRITICAL EVALUATION

The collected experimental data for HCFC-123 are summarized in Tables I and II for the thermal conductivity and in Tables III and IV for the viscosity. It is found that the pressure range covered with the existing data exceeds by far the region in which heat pumps and refrigeration cycles operate. On the other hand, the temperature range does not cover the critical and supercritical regions, since the critical temperature of HCFC-123 456.831 K is appreciably high.

In this section, the comparison and critical evaluation of available experimental data are discussed for each physical state in the following order: (1) saturated liquid (LS), (2) compressed liquid (LP), (3) vapor at atmospheric pressure (GA), (4) saturated vapor (GS), and (5) superheated vapor (GP).

To compare the existing data with each other, empirical temperature dependence and temperature–pressure dependence correlations have been performed tentatively for each physical state independently with the aid of simple polynomial equations of $T$ or $T$ and $P$. The scattering of data, temperature and pressure dependences of $\lambda$ and $\eta$ were compared with each other.

### 4.1. Thermal Conductivity of HCFC-123

#### *4.1.1. Saturated Liquid*

More than seven sets of experimental data have been reported for the saturated liquid thermal conductivity of HCFC-123 in the temperature range from 159 to 354 K: those of Tanaka et al. [12], Yata et al. [14, 16], Gross et al. [17, 22], Shankland [18], Kobayashi et al. [19], Ueno et al.

**Table I.** Liquid Thermal Conductivity Data for HCFC-123 (2,2-Dichloro-1,1,1-trifluoroethane)[a]

| First author | Ref. No. | Year | Method | Temperature | | Pressure | | Uncertainty (%) | Sample Purity (%) | No. of Data |
|---|---|---|---|---|---|---|---|---|---|---|
| | | | | Range (K) | Uncertainty (K) | Range (MPa) | Uncertainty (MPa) | | | |
| Tanaka | 12 | 1988 | HW | 283–323 | | 0.1–200 | | 1 | 99.9 | 36 |
| Kobayashi | 13 | 1989 | HW | 273–353 | 0.08 | 1–40 | 0.035 | 0.5 | 99.8 | 116(25) |
| Yata | 14 | 1989 | HW | 263–344 | 0.02 | 0.2–30 | | 1 | 99.8 | 20 |
| Fukushima | 15 | 1989 | HW | 294–333 | | 0.1–4.8 | | 2 | | 44(10) |
| Yata | 16 | 1990 | HW | 252–373 | 0.02 | 0.5–10 | | 1 | 99.9 | 32 |
| Gross | 17 | 1990 | HW | 254–354 | | Sat. | 0.005–0.015 | 2 | 99.5 | 15 |
| Shankland | 18 | 1990 | HW | 308–341 | | Sat. | | 1 | | 8 |
| Kobayashi | 19 | 1990 | HW | 194–353 | 0.05 | 1–30 | 0.07 | 0.5 | 99.8 | 36 |
| Ueno | 20 | 1990 | HW | 194–353 | 0.05 | 1–30 | 0.07 | 0.5 | 99.8 | 36 |
| Ueno | 21 | 1991 | HW | 194–353 | | 1–30 | 0.07 | 0.5 | 99.8 | 36 |
| Gross | 22 | 1992 | HW | 254–354 | | 0.1–6.2 | | 1.6 | 99.8 | 42 |
| Assael | 23 | 1993 | HW | 253–333 | | Sat.–28.3 | | 1.6 | 99.8 | 36 |
| Venart | 24 | 1993 | HW | 220–360 | | 0.1–40 | | | | 460 |
| Tsvetkov | 25 | 1994 | TCC | 159–291 | 0.001 | Sat. | | 2–3 | 95 | 19 |

[a] HW, transient hot-wire method; TCC, transient coaxial-cylinder method; sat., saturated vapor pressure.

**Table II.** Vapor Thermal Conductivity Data for HCFC-123[a]

| First author | Ref. No. | Year | Method | Temperature | | Pressure | | Uncertainty (%) | Sample Purity (%) | No. of Data |
|---|---|---|---|---|---|---|---|---|---|---|
| | | | | Range (K) | Uncertainty (K) | Range (MPa) | Uncertainty (MPa) | | | |
| Richard | 26 | 1989 | HW | 306–328 | | 0.1–sat. | | | | 6 |
| Gross | 17 | 1990 | HW | 305–364 | | Sat. | 0.005–0.015 | 2 | 99.5 | 12 |
| Tanaka | 27 | 1991 | CC | 313–343 | 0.05 | 0.1–sat. | 0.04 | 2 | 99.9 | 32 |
| Shankland | 18 | 1990 | HW | 306–328 | | 0.1–sat. | | 3 | | 6 |
| Ueno | 28 | 1991 | HW | 323–443 | 0.05 | Sat. | 0.035 | 0.5 | 99.8 | 27 |
| Yamamoto | 29 | 1992 | HW | 313–373 | | 0.1–sat. | | | | 13 |
| Gross | 22 | 1992 | HW | 305–365 | | 0.1–6 | | 2 | 99.8 | 32 |

[a] HW, transient hot-wire method; CC, steady-state coaxial-cylinder method; sat., saturated vapor pressure.

**Table III.** Liquid Viscosity Data for HCFC-123 (2,2-Dichloro-1,1,1-trifluoroethane)[a]

| First author | Ref. No. | Year | Method | Temperature | | Pressure | | Uncertainty (%) | Sample Purity (%) | No. of Data |
|---|---|---|---|---|---|---|---|---|---|---|
| | | | | Range (K) | Uncertainty (K) | Range (MPa) | Uncertainty (MPa) | | | |
| Ohta | 30 | 1988 | FC | 293–313 | 0.03 | 0.1–98 | 0.1 | 2 | 99.8 | 12 |
| Kumagai | 31 | 1990 | C | 273–353 | 0.03 | Sat. | | 0.5 | 99.6 | 9 |
| Shankland | 18 | 1990 | C | 277–327 | 0.02 | Sat. | | 1 | 99.5 | 12 |
| Diller | 32, 33 | 1991 | OC | 170–320 | | Sat. | | 2 | | 52 |
| | | | | 200–300 | | 3–33 | | | | |
| Okubo | 34, 35 | 1992 | C | 233–418 | | 1–20 | | 1.2 | 99.77 | 62 |
| Peckover | 36 | 1993 | RB | 253–333 | 0.002 | Sat. | 0.06 | 0.5 | | 9 |
| Lagasse | 36 | 1993 | RB | 253–333 | 0.002 | Sat. | 0.06 | 0.5 | | 9 |

[a] FC, falling-cylinder method; C, capillary method; OC, torsionally oscillating-crystal method; RB, rolling-ball method; sat., saturated vapor pressure.

**Table IV.** Vapor Viscosity Data for HCFC-123[a]

| First author | Ref. No. | Year | Method | Temperature | | Pressure | | Uncertainty (%) | Sample Purity (%) | No. of Data |
|---|---|---|---|---|---|---|---|---|---|---|
| | | | | Range (K) | Uncertainty (K) | Range (MPa) | Uncertainty (MPa) | | | |
| Takahashi | 37 | 1990 | OD | 323–423 | 0.01 | 0.1–1.96 | 0.03–0.5 | 0.3 | 99.6 | 47 |
| Nabizadeh | 38, 39 | 1990 | OD | 303–423 | | 0.1–2 | | 0.5 | | 31 |

[a] OD, oscillating-disk method.

[20, 21], Assael and Karagiannidis [23], and Tsvetkov et al. [25]. Among these data, those of Kobayashi et al. [19] and Ueno et al. [20, 21] are substantially the same data which have been reported by one research group. All measurements except for those of Tsvetkov et al. [25] were obtained with the transient hot-wire method. It is very difficult to measure the thermal conductivity just at saturation pressures. Therefore, most of the data mentioned above were obtained by extrapolation of the liquid thermal conductivity at high pressures along the isotherms down to the saturation pressures. Almost all data agree within $\pm 2\%$.

Tsvetkov et al. [25] measured 19 data from 159 to 291 K near the saturation line by a transient coaxial-cylinder apparatus. The asserted uncertainty of the measurements is 2–3%. However, it should be noted that the sample fluid used was an isomeric blend of 95% HCFC-123 and 5% HCFC-123a ($CHClF\text{-}CClF_2$).

*4.1.2. Compressed Liquid*

Tanaka et al. [12], Yata et al. [14, 16], Fukushima and Watanabe [15], Ueno et al. [20, 21], Kobayashi et al. [19], Gross et al. [17, 22], Assael and Karagiannidis [23], and Venart [24] measured the compressed liquid thermal conductivity by the transient hot-wire method in the temperature ranges from 193 to 373 K and the pressure ranges from 0.1 to 200 MPa. The data of Venart [24] were obtained recently. They reported in their previous paper [43] that strong fluid radiation effects have been observed in the measurements of thermal conductivity, thermal diffusivity, and isobaric heat capacitiy of HCFC-123 by the transient hot-wire method in both liquid and vapor phases which require substantial corrections. On the other hand, Assael and Karagiannidis [23] reported that no radiation correction was necessary for the temperature range from 253 to 333 K and the pressure range up to 20 MPa. Other researchers did not discuss this problem. The collected data mentioned above were compared with each other in terms of an empirical equation given by Ueno et al. [20, 21] as a tentative standard. It is found that the existing data are mutually consistent within $\pm 3\%$. The data of Assael and Karagiannidis [23], Fukushima and Watanabe [15], Tanaka et al. [12], and Yata et al. [14, 16] agree with the equation of Ueno et al. [20, 21] within $\pm 1.5\%$, whereas those of Venart [24] and Gross et al. [17, 22] are systematically a little higher than the equation by about 3 and 2%, respectively.

*4.1.3. Vapor at Atmospheric Pressure*

Four sets of data are available in the literature at temperatures from 290 to 373 K: those of Tanaka et al. [27], Gross et al. [22], Yamamoto

et al. [29], and Venart [24]. Among them, the data of Tanaka et al. [27] were measured with a steady-state coaxial-cylinder apparatus. Although the absolute values of these data agree within 1%, the temperature coefficient $(\partial\lambda/\partial T)_P$ of Tanaka et al. [27] is a little higher than those of Gross et al. [22] and Yamamoto et al. [29].

*4.1.4. Saturated Vapor*

Only three sets of experimental data could be found in the literature: those of Richard and Shankland [18, 26], Gross et al. [17, 22], and Ueno et al. [28]. The differences between the vapor data at atmospheric pressure and at the saturation pressure are small since the temperature range covered by experimental data is far from the critical point. The experimental results measured by Richard and Shankland [18, 26] are found to be larger than those of Gross et al. [17, 22] by 3–8%.

*4.1.5. Superheated Vapor*

Only four sets of data are available for the superheated vapor of HCFC-123: those of Tanaka et al. [27], Gross et al. [17, 22], Yamamoto et al. [29], and Venart [24]. Among them, the data of Tanaka et al. [27] were obtained with a steady-state coaxial-cylinder apparatus, whereas other data were measured by the transient hot-wire method. These data were compared with the aid of an empirical temperature–pressure dependence correlating equation made by Tanaka et al. [27] as a tentative standard. It is found that these four sets of data agree mutually within 4% in the temperature range from 304 to 353 K. However, the deviations reach about 10% near the saturation pressures in the temperature range from 353 to 373 K. It is possible that the effect of natural convection is included in the data obtained with a steady-state coaxial-cylinder apparatus. The pressure coefficients $(\partial\lambda/\partial P)_T$ of these data contradict each other. More precise measurements are urgently needed in the vapor phase.

## 4.2. Viscosity of HCFC-123

*4.2.1. Saturated Liquid*

Five sets of data are available in the literature: those of Shankland [18], Kumagai and Takahashi [31], Diller et al. [32, 33], Peckover [36], and Lagasse [36]. Shankland [18] measured 12 data from 277 to 327 K by a coiled capillary-type viscometer. Kumagai and Takahashi [31] measured nine data from 273 to 353 K using a straight capillary viscometer. Diller et al. [32, 33] obtained 23 data from 170 to 320 K with a torsionally oscillating-quartz viscometer. Peckover [36] and Lagasse [36] measured nine

data separately at the same temperatures from 253 to 333 K by the same rolling-ball viscometer. The data of Peckover [36] are 3% higher systematically than Kumagai and Takahashi [31] throughout the temperature range. On the other hand, the results of Lagasse [36] deviate more than +5 to +9% from those of Kumagai and Takahashi [31] below 283 K, although these data agree within about 1.5% in the higher-temperature range above 293 K. The data of Shankland [18] are systematically higher than those of Kumagai and Takahashi [31] by about 13%. The data of Diller et al. [32, 33] agree well with those of Kumagai and Takahashi [31] throughout the experimental condition.

*4.2.2. Compressed Liquid*

Ohta [30], Diller et al. [32, 33], and Okubo et al. [34, 35] measured the compressed liquid viscosity of HCFC-123. We compared these data with each other using an empirical correlating equation presented by Okubo et al. [34, 35] as a tentative standard. It is found that the data of Diller et al. [32, 33] at 250 and 300 K are systematically larger than those of Okubo et al. [34, 35] by 4–5%, whereas the data of Ohta [30] agree with Okubo et al. [34, 35] within 2% at 293 and 313 K.

*4.2.3. Vapor at Atmospheric Pressure*

Only two sets of measurements are reported for the vapor viscosity at atmospheric pressure: those of Takahashi et al. [37] and Nabizadeh and Mayinger [38, 39]. Takahashi et al. [37] measured five data from 323 to 423 K with an oscillating-disk viscometer. Nabizadeh and Mayinger [38, 39] reported six data from 303 to 423 K measured by an oscillating-disk viscometer. These data agree quite well within 1%.

*4.2.4. Saturated Vapor*

No experimental data could be found in the literature at present.

*4.2.5. Superheated Vapor*

Only two sets of data are available for superheated vapor viscosity of HCFC-123, those of Takahashi et al. [37] and Nabizadeh and Mayinger [38, 39]. We compared these data using an empirical correlating equation adopted in the thermophysical property tables published by JAR [5]. It is found that these two data agree reasonablly within 2% from 332 to 373 K, although the data of Nabizadeh and Mayinger [38, 39] become higher than those of Takahashi et al. [37] by 2–4% at 423 K above 1 MPa. The pressure coefficients $(\partial\eta/\partial P)_T$ of these data are definitely inconsistent in the region above 373 K and 0.5 MPa. In this connection the data of Nabizadeh

and Mayinger [38, 39] for the superheated vapor viscosity of HCFC-142b have also been compared with those of Takahashi et al. [40]. It is found that the data of Nabizadeh and Mayinger [38, 39] become higher than those of Takahashi et al. [40] by 2–7% at 373 K in the higher-pressure range above 0.8 MPa, although these data agree quite well, within 1%, from 304 to 333 K at low pressures. A similar behavior is also reported for HFC-134a [4]. The eminent difference of $(\partial\eta/\partial P)_T$ at high temperatures and high pressures may be ascribed to the intrinsic characteristics of their oscillating-disk viscometers.

## 5. RESULTS OF RESIDUAL CONCEPT CORRELATION

### 5.1. Thermal Conductivity

#### *5.1.1. Dilute-Gas Function*

Since zero-density data of the thermal conductivity are lacking, the data measured at atmospheric pressure or below were used for the correlation. In view of the scattering of the data this is justified. The resulting error lies within the uncertainty of the measurements. The data sets of Gross et al. [17, 22] and Yamamoto et al. [29] were selected as the primary data. It turned out that the temperature dependence of the gaseous

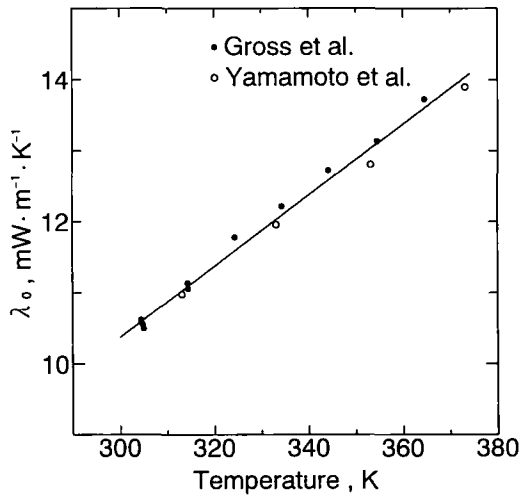


**Fig. 1.** The zero-density thermal conductivity of HCFC-123 as a function of temperature. The solid line represents the values as calculated from Eq. (6).

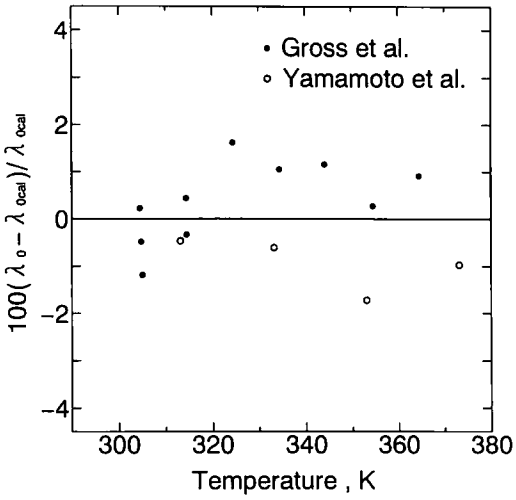


Fig. 2. Percentage deviations of the primary zero-density thermal conductivity data from the final correlation.

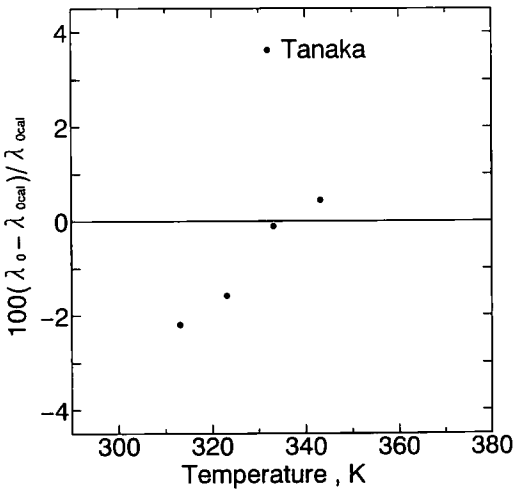


Fig. 3. Percentage deviations of the secondary zero-density thermal conductivity data from the final correlation.

thermal conductivity at atmospheric pressure could be represented by a straight line as follows:

$$\lambda_0(T) = -4.646772 + 5.006573 \times 10^{-2} T \tag{6}$$

with a mean deviation of 0.82%, a maximum deviation of 1.72%, and an uncertainty of 2%. The equation is valid at 253–373 K. The dilute-gas function of the thermal conductivity of HCFC-123 is shown in Fig.1 together with the selected experimental data. The corresponding deviations are plotted in Figs. 2 and 3 for the primary data and the secondary data, which were not used for the present correlation, respectively. It is found that the data could be fitted with an uncertainty of less than 2%.

### *5.1.2. Excess Function*

The excess thermal conductivity $\Delta\lambda_R(\rho)$ can be calculated by subtracting the corresponding dilute-gas value $\lambda_0(T)$ and the critical enhancement term $\Delta\lambda_c(\rho, T)$ from the actual thermal conductivity $\lambda(\rho, T)$ at the same temperature. For HCFC-123, no experimental data are available so close to the critical point and the critical enhancement can be neglected.

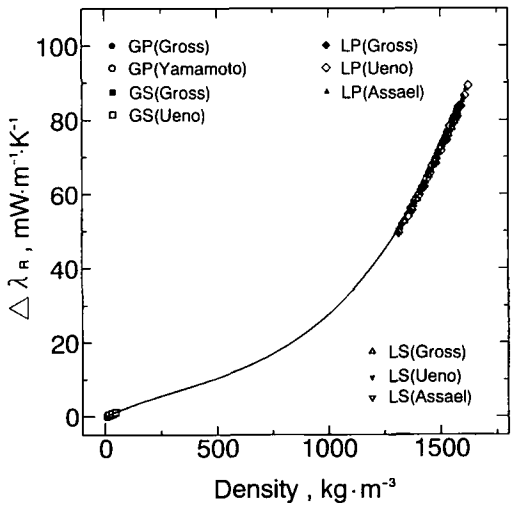


**Fig. 4.** The excess thermal conductivity of HCFC-123 as a function of density. The solid line represents the values as calculated from Eq. (7).

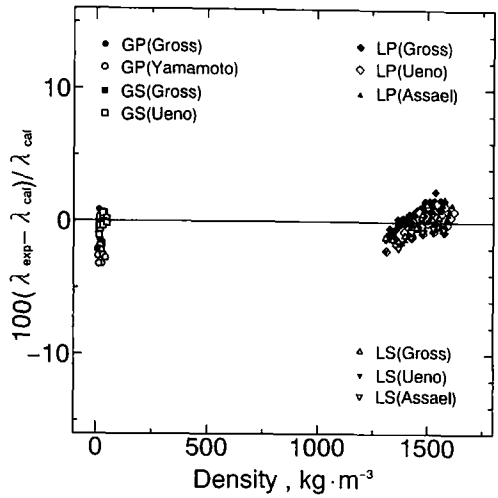


**Fig. 5.** Percentage deviations of primary thermal conductivity data from the final correlation.

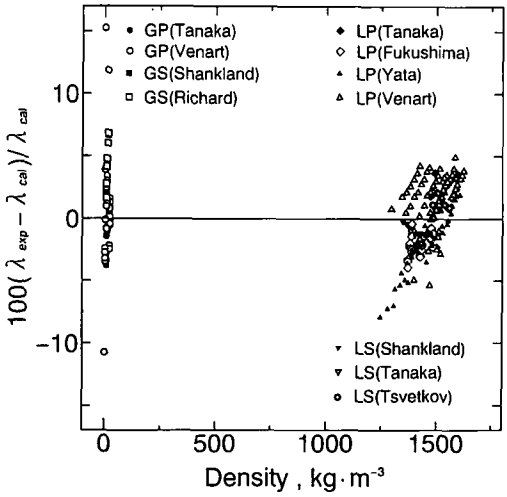


**Fig. 6.** Percentage deviations of secondary thermal conductivity data from the final correlation.

The excess function is based on the measurements of Gross et al. [17, 22], Ueno et al. [20, 21], and Assael and Karagiannidis [23] in the liquid phase and of Ueno et al. [28], Gross et al. [17, 22], and Yamamoto et al. [29] in the vapor phase. The excess thermal conductivity can be represented as a function of the density by a third-order polynomial as follows:

$$\Delta\lambda_R(\rho) = 2.722289 \times 10^{-2}\rho - 2.581605 \times 10^{-5}\rho^2 + 2.626926 \times 10^{-8}\rho^3 \quad (7)$$

$\Delta\lambda_R$, $mW \cdot m^{-1} \cdot K^{-1}$, $253 \leqslant T \leqslant 373$ K, and $0 \leqslant \rho \leqslant 1623$ $kg \cdot m^{-3}$, with a mean deviation of 0.93%, a maximum deviation of 3.23%, and an uncertainty of 3%. The parameter values for an optimal respresentation of the selected data were obtained from a least-squares fit. The residual themal conductivity is shown in Fig. 4 as a function of density according to Eq. (7). Percentage deviations of the primary data sets from the correlation and

**Table V.** Comparison of Experimental Thermal Conductivity Data with the Correlation

| First author | Ref. No. | Data points | $T_{min}$ (K) | $T_{max}$ (K) | $P_{min}$ (MPa) | $P_{max}$ (MPa) | Mean dev. (%) | Max. dev. (%) |
|---|---|---|---|---|---|---|---|---|
| Primary data | | | | | | | | |
| Gross (GP) | 21 | 22 | 314 | 364 | 0.1 | 0.6 | 1.25 | 2.61 |
| Yamamoto (GP) | 27 | 9 | 313 | 373 | 0.1 | 0.7 | 2.52 | 3.23 |
| Gross (GS) | 16 | 6 | 305 | 364 | 0.1 | 0.6 | 0.78 | 2.10 |
| Ueno (GS) | 26 | 13 | 323 | 373 | 0.2 | 0.8 | 0.42 | 1.04 |
| Gross (LP) | 21 | 42 | 254 | 354 | 0.01 | 6.2 | 0.97 | 2.31 |
| Ueno (LP) | 18, 19, 20 | 24 | 253 | 353 | 1.0 | 30.0 | 0.78 | 2.17 |
| Assael (LP) | 22 | 36 | 253 | 333 | 0.1 | 28.3 | 0.69 | 1.88 |
| Gross (LS) | 16 | 15 | 255 | 354 | 0.01 | 0.5 | 0.65 | 1.43 |
| Ueno (LS) | 18, 19, 20 | 6 | 253 | 353 | 0.01 | 0.5 | 1.23 | 2.16 |
| Assael (LS) | 22 | 5 | 253 | 333 | 0.01 | 0.3 | 0.90 | 1.93 |
| Secondary data | | | | | | | | |
| Tanaka (GP) | 25 | 24 | 313 | 343 | 0.1 | 0.4 | 1.42 | 3.81 |
| Venart (GP) | 23 | 27 | 289 | 360 | 0.02 | 0.4 | 3.00 | 15.3 |
| Shankland (GS) | 17 | 6 | 306 | 328 | 0.1 | 0.2 | 4.38 | 6.67 |
| Richard (GS) | 24 | 6 | 306 | 328 | 0.1 | 0.2 | 4.38 | 6.84 |
| Ohta (LP) | 11 | 8 | 283 | 323 | 0.1 | 25.1 | 1.92 | 3.65 |
| Fukushima (LP) | 14 | 37 | 294 | 333 | 0.1 | 4.6 | 1.99 | 3.92 |
| Yata (LP) | 13, 15 | 47 | 262 | 374 | 0.2 | 30.8 | 2.34 | 7.87 |
| Venart (LP) | 23 | 52 | 260 | 360 | 0.1 | 30.0 | 2.14 | 5.35 |
| Shankland (LS) | 17 | 8 | 308 | 342 | 0.1 | 0.4 | 0.92 | 1.75 |
| Tanaka (LS) | 11 | 4 | 283 | 323 | 0.05 | 0.2 | 2.92 | 4.92 |
| Tsvetkov (LS) | 46 | 5 | 260 | 291 | 0.02 | 0.07 | 0.94 | 1.16 |

those of the secondary data sets are shown in Figs. 5 and 6, respectively, (also see Table V). These comparisons are made on the basis of the total thermal conductivity $\lambda(\rho, T)$ rather than the residual thermal conductivity $\Delta\lambda_R(\rho)$.

## 5.2. Viscosity

### *5.2.1. Dilute-Gas Function*

Since the zero-density data of the viscosity are lacking, the data measured at atmospheric pressure or below by Takahashi et al. [37] and Nabizadeh and Mayinger [38, 39] were used to determine the zero-density function. Due to the scattering of the data sets, the resulting error lies within the uncertainties of the measurements.

According to the rigorous kinetic theory of gases, the viscosity of a dilute gas is given by the Chapman–Enskog equation [41]. Nabizadeh and Mayinger [38, 39] determined the optimum values of the scaling factors $\varepsilon/k$ and $\sigma$ from their viscosity data for the collision integral given by Kestin et al. [42] as follows:

$$\varepsilon/k = 275.16 \text{ K}, \qquad \sigma = 0.5909 \text{ nm}$$

Similarly, Takahashi et al. [37] obtained the following scaling parameters for the collision integral based on the Lennard–Jones 12–6 potential [41];

$$\varepsilon/k = 340 \text{ K}, \qquad \sigma = 0.56 \text{ nm}$$

It was found that the Chapman–Enskog equation and these scaling parameters provide a good representation of their data, with a mean deviation of 0.3%. Thus, the present correlation of dilute gas function was made based on the measurements of Takahashi et al. [37], and Nabizadeh and Mayinger [38, 39] and the values calculated from the Chapman-Enskog equation at lower temperatures, below 303 K.

$$\eta_0(T) = -2.273638 + 5.099859 \times 10^{-2} T - 2.402786 \times 10^{-5} T^2 \qquad (8)$$

with a mean deviation of 0.16%, a maximum deviation of 0.34%, and an uncertainty of 0.3%. The dilute-gas function of the viscosity is shown in Fig. 7 together with the experimental data of Takahashi et al. [37] and Nabizadeh and Mayinger [38, 39]. The relative deviations are plotted in Fig. 8. Equation (8) is valid at temperatures from 253 to 423 K, but it can be extrapolated outside this temperature range with a modest loss of accuracy.

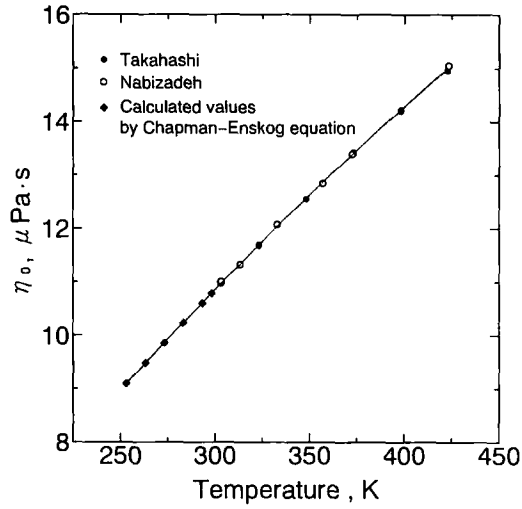


**Fig. 7.** The zero-density viscosity of HCFC-123 as a function of temperature. The solid line represents the values as calculated from Eq. (8).

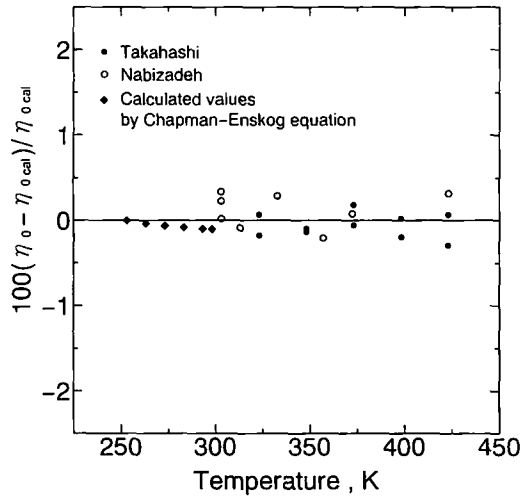


**Fig. 8.** Percentage deviations of the primary zero-density viscosity data from the final correlation.

*5.2.2. Excess Function*

The excess viscosity $\eta_R(\rho)$ can be calculated by subtracting the corresponding dilute-gas value $\eta_0(T)$ and the initial density-dependence term $\eta_1(T)\rho$ from the actual viscosity $\eta(\rho, T)$ at the same temperature. The critical enhancement can be neglected since no experimental data are available close to the critical point.

The initial density-dependence term $\eta_1(T)\rho$ was determined first based on the vapor viscosity values at low densities measured by Takahashi et al. [37] as follows:

$$\eta_1(T) = -2.226486 \times 10^{-2} + 5.550623 \times 10^{-5} T \tag{9}$$

where $\eta_1$ is in $\mu$Pa · s, and $298 \leqslant T \leqslant 423$ K.

The excess function $\Delta\eta_R(\rho)$ is based on the measurements of Kumagai and Takahashi [31], Diller et al. [32, 33], and Okubo and Nagashima [34, 35] in the liquid phase and of Takahashi et al. [37] in the vapor phase. The low-temperature data (200 and 250 K) of Diller et al. [32, 33] were omitted.

The steep increase in the viscosity at very high densities made it impossible to correlate the excess viscosity by an ordinary polynomial in density with sufficient accuracy. A variety of functional forms was tested for the correlation. The sixth-degree polynomial functions gave a quite satisfactory fit to the selected data in both gaseous and liquid phases. However, we were unable to eliminate some systematic error patterns in the intermediate-density region. Instead, we used a hyperbolic function which turned out to be successful in reproducing the extreme gradient of the viscosity at very high densities. It was found that a third-degree polynomial combined with a hyperbolic term [4, 6, 7, 9] could represent best the excess viscosities as extracted from the above selected data as follows:

$$\Delta\eta_R(\rho) = \frac{a_0}{\rho - \rho_0} + \frac{a_0}{\rho_0} + a_1\rho + a_2\rho^2 + a_3\rho^3 \tag{10}$$

$$\rho_0 = 1.828263 \times 10^3 \qquad a_0 = -3.222951 \times 10^5$$

$$a_1 = -1.009812 \times 10^{-1}, \qquad a_2 = 6.161902 \times 10^{-5}$$

$$a_3 = -8.84048 \times 10^{-8}$$

where $\Delta\eta_R$ is in $\mu$Pa · s, $253 \leqslant T \leqslant 423$ K, and $0 \leqslant \rho \leqslant 1608$ kg · m$^{-3}$, with a mean deviation of 1.17%, a maximum deviation of 5.16%, and an uncertainty of 5%. Several supplementary data were added to combine the dilute-gas region and the compressed liquid region smoothly. A tem-

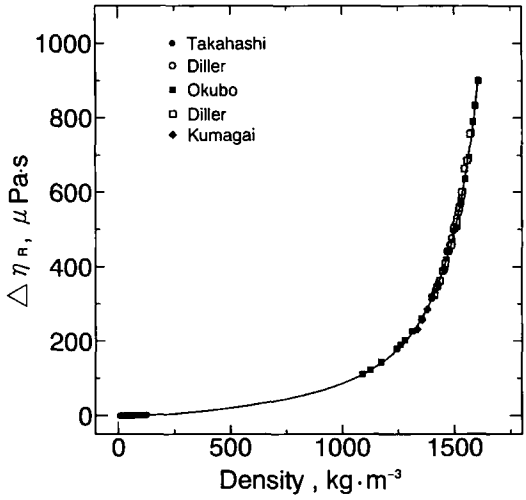


**Fig. 9.** The excess viscosity of HCFC-123 as a function of density. The solid line represents the values as calculated from Eq. (10).

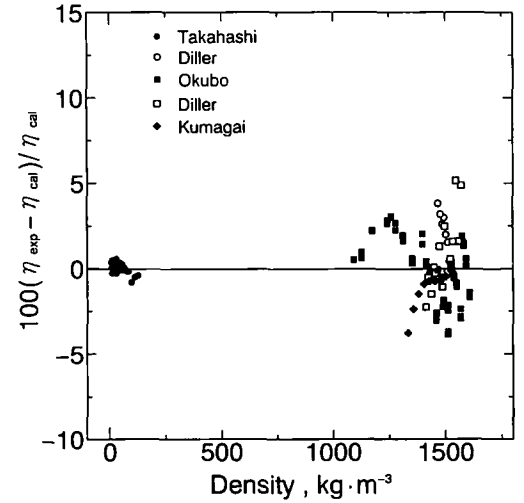


**Fig. 10.** Percentage deviations of primary viscosity data from the final correlation.

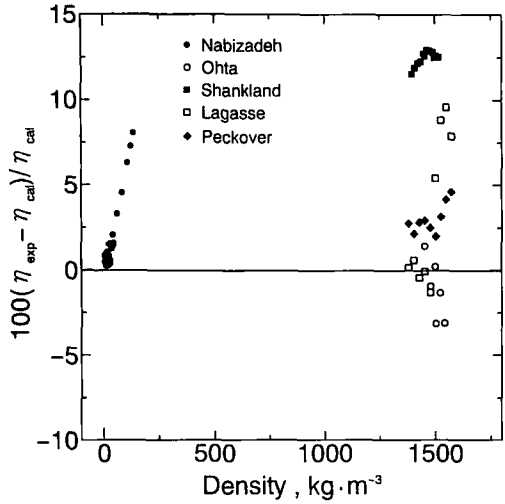


**Fig. 11.** Percentage deviations of secondary viscosity data from the final correlation.

perature dependence was not included since the experimental data are still scarce and somewhat contradictory at present. The adjustable parameters were obtained from a nonlinear fit of weighted least squares.

The excess viscosity of HCFC-123 as calculated from Eq. (10) is illustrated in Fig. 9. Percentage deviations of the selected data sets from the correlation, (Table VI) and those which were not used for the correlation,

**Table VI.** Comparison of Experimental Viscosity Data with the Correlation

| First author | Ref. No. | Data points | $T_{min}$ (K) | $T_{max}$ (K) | $P_{min}$ (MPa) | $P_{max}$ (MPa) | Mean dev. (%) | Max. dev. (%) |
|---|---|---|---|---|---|---|---|---|
| Primary data | | | | | | | | |
| Takahashi (GP) | 35 | 37 | 323 | 423 | 0.1 | 2.0 | 0.26 | 0.81 |
| Diller (LP) | 30, 31 | 9 | 300 | 300 | 3.5 | 32.2 | 1.89 | 3.83 |
| Okubo (LP) | 32, 33 | 54 | 253 | 418 | 1.1 | 20.7 | 1.52 | 3.88 |
| Diller (LS) | 30, 31 | 14 | 255 | 320 | 0.1 | 1.9 | 1.70 | 5.16 |
| Kumagai (LS) | 29 | 9 | 273 | 353 | 0.3 | 4.9 | 1.26 | 3.77 |
| Secondary data | | | | | | | | |
| Nabizadeh (GP) | 36, 37 | 23 | 313 | 423 | 0.1 | 2.0 | 1.94 | 8.08 |
| Tanaka (LP) | 28 | 6 | 293 | 313 | 9.9 | 29.5 | 1.68 | 3.13 |
| Shankland (LS) | 17 | 12 | 278 | 328 | 0.4 | 2.4 | 12.5 | 13.0 |
| Lagasse (LS) | 34 | 9 | 253 | 333 | 0.1 | 2.9 | 3.82 | 9.61 |
| Peckover (LS) | 34 | 9 | 253 | 333 | 0.1 | 2.9 | 3.02 | 4.62 |

are depicted in Figs. 10 and 11, respectively. All deviations are calculted in terms of the total viscosity $\eta(\rho, T)$ rather than in terms of only the residual part $\Delta\eta_R(\rho)$.

## 6. THE CRITICAL REGION

As shown in Tables I–IV no experimental data are available in the literature near and over the critical point for the thermal conductivity and the viscosity at present. Reliable crossover equations of state are still missing. Therefore the critical enhancement term $\Delta\lambda_c(\rho, T)$ was not considered here. Detailed information about the calculation of the thermal conductivity in the critical region is given by Sengers et al. [44–46] and Krauss et al [4].

## 7. THERMAL DIFFUSIVITY

The thermal diffusivity $a$ is defined by the thermal conductivity $\lambda$, the isobaric specific heat capacity $c_p$, and the density $\rho$ as follows:

$$a = \lambda/(c_p\rho) \tag{11}$$

The thermal diffusivity can be measured by several techniques, utilizing different ways of perturbing the fluid, namely, the dynamic light scattering, the interferometric technique, and the simultaneous measurement of the thermal conductivity and the thermal diffusivity with the transient hot-wire technique.

Only two sets of measurements are available in the literature for the thermal diffusivity of HCFC-123. Ibreighith et al. [47] measured the thermal diffusivity in the liquid phase over the temperature range between 273 and 443 K and at pressures 2.0, 3.5, and 5.0 MPa. The principle of the measurement is based on analyzing the Rayleigh spectrum by use of the photon correlation spectroscopy. At temperatures above 443 K, HCFC-123 starts to decompose. As shown in Fig. 12, the measured thermal diffusivity of the liquid HCFC-123 decreases almost linearly with temperature. The effect of pressure on the thermal diffusivity is quite small. For comparison, the data of CFC-11 are included together with the results of Venart [24] for liquid HCFC-123 at 5 MPa. According to Ibreighith et al. [47] the thermal diffusivity of HCFC-123 is about 25% lower than CFC-11. Both curves have approximately the same slope. The reported accuracy of the thermal diffusivity is better than 1.2%.

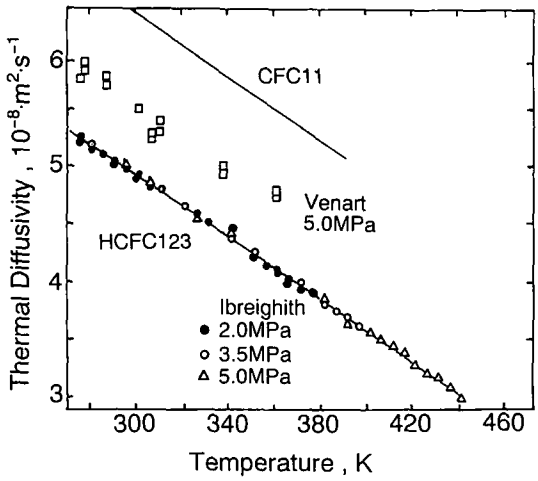


**Fig. 12.** Temperature dependence of the liquid thermal diffusivity of HCFC-123 measured by Ibreighith et al. [47].

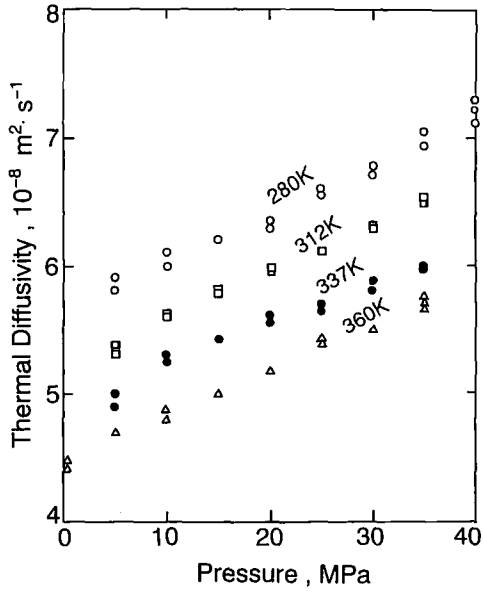


**Fig. 13.** Pressure dependences of the liquid thermal diffusivity of HCFC-123 measured by Venart [24].

Venart [24] measured the thermal diffusivity of HCFC-123 between 198 and 358 K at pressures up to 40 MPa along 11 isotherms in both the liquid and the vapor phases. The measurements were carried out by the transient hot-wire apparatus simultaneously with the thermal conductivity and the isobaric specific heat capacity. Several isotherms are plotted against pressure in Fig. 13. Judging from Fig. 12, large discrepancies, more than 10%, are found between the results of Ibreighith et al. [47] and those of Venart [24], although the temperature dependences of the thermal diffusivity are approximately consistent each other.

The thermal diffusivity $a$ is defined by Eq. (11). Therefore it can be calculated from the thermal conductivity with the aid of the isobaric specific heat capacity and the density, which can be obtained from the equation of state by Younglove and McLinden [3].

## 8. TABULATIONS

The final representations of the thermal conductivity and the viscosity of HCFC-123 are given in Tables VII–IX.

**Table VII.** Thermal Conductivity and Viscosity of HCFC-123 Along the Saturation Line

| Temperature (K) | Pressure (MPa) | Density ($kg \cdot m^{-3}$) | | Thermal conductivity ($mW \cdot m^{-1} \cdot K^{-1}$) | | Viscosity ($\mu Pa \cdot s$) | |
|---|---|---|---|---|---|---|---|
| | | $\rho'$ | $\rho''$ | $\lambda'$ | $\lambda''$ | $\eta'$ | $\eta''$ |
| 260 | 0.179 | 1557.7 | 1.286 | 87.42 | 8.405 | 670.0 | 9.346 |
| 265 | 0.229 | 1545.8 | 1.614 | 86.04 | 8.665 | 627.1 | 9.534 |
| 270 | 0.289 | 1533.8 | 2.007 | 84.68 | 8.926 | 587.8 | 9.721 |
| 273.15 | 0.334 | 1526.2 | 2.292 | 83.82 | 9.091 | 564.7 | 9.838 |
| 275 | 0.362 | 1521.7 | 2.474 | 83.32 | 9.188 | 551.7 | 9.906 |
| 280 | 0.449 | 1509.4 | 3.025 | 81.98 | 9.454 | 518.4 | 10.09 |
| 285 | 0.553 | 1497.1 | 3.671 | 80.66 | 9.722 | 487.8 | 10.27 |
| 290 | 0.674 | 1484.6 | 4.422 | 79.34 | 9.992 | 459.4 | 10.45 |
| 298.15 | 0.919 | 1463.9 | 5.906 | 77.22 | 10.44 | 417.6 | 10.74 |
| 300 | 0.983 | 1459.2 | 6.292 | 76.74 | 10.54 | 408.7 | 10.80 |
| 305 | 1.174 | 1446.2 | 7.438 | 75.46 | 10.82 | 386.1 | 10.98 |
| 310 | 1.394 | 1433.1 | 8.742 | 74.19 | 11.11 | 364.9 | 11.15 |
| 315 | 1.644 | 1419.8 | 10.22 | 72.92 | 11.40 | 345.2 | 11.32 |
| 320 | 1.929 | 1406.4 | 11.89 | 71.67 | 11.69 | 326.8 | 11.49 |
| 325 | 2.251 | 1392.7 | 13.77 | 70.43 | 12.00 | 309.6 | 11.66 |
| 330 | 2.612 | 1378.8 | 15.88 | 69.19 | 12.30 | 293.5 | 11.83 |
| 335 | 3.017 | 1364.7 | 18.24 | 67.96 | 12.61 | 278.4 | 12.00 |
| 340 | 3.468 | 1350.4 | 20.87 | 66.74 | 12.93 | 264.1 | 12.17 |

**Table VII.** *(Continued)*

| Temperature (K) | Pressure (MPa) | Density ($kg \cdot m^{-3}$) | | Thermal conductivity ($mW \cdot m^{-1} \cdot K^{-1}$) | | Viscosity ($\mu Pa \cdot s$) | |
|---|---|---|---|---|---|---|---|
| | | $\rho'$ | $\rho''$ | $\lambda'$ | $\lambda''$ | $\eta'$ | $\eta''$ |
| 345 | 3.969 | 1335.7 | 23.80 | 65.53 | 13.26 | 250.7 | 12.34 |
| 350 | 4.522 | 1320.8 | 27.04 | 64.32 | 13.59 | 238.1 | 12.52 |
| 355 | 5.132 | 1305.5 | 30.64 | 63.12 | 13.94 | 226.2 | 12.69 |
| 360 | 5.802 | 1289.9 | 34.61 | 61.92 | 14.29 | 214.9 | 12.87 |
| 365 | 6.535 | 1273.9 | 39.01 | 60.72 | 14.65 | 204.3 | 13.05 |
| 370 | 7.336 | 1257.5 | 43.86 | 59.52 | 15.02 | 194.2 | 13.25 |
| 375 | 8.207 | 1240.6 | 49.21 | 58.33 | 15.41 | 184.6 | 13.45 |
| 380 | 9.152 | 1223.2 | 55.12 | 57.13 | 15.81 | 175.4 | 13.66 |
| 385 | 10.18 | 1205.2 | 61.64 | 55.92 | 16.22 | 166.7 | 13.88 |
| 390 | 11.28 | 1186.5 | 68.85 | 54.71 | 16.64 | 158.4 | 14.13 |
| 395 | 12.47 | 1167.1 | 76.83 | 53.50 | 17.08 | 150.4 | 14.39 |
| 400 | 13.76 | 1146.8 | 85.68 | 52.27 | 17.54 | 142.8 | 14.69 |
| 405 | 15.13 | 1125.6 | 95.52 | 51.02 | 18.02 | 135.4 | 15.02 |
| 410 | 16.61 | 1103.1 | 106.5 | 49.76 | 18.52 | 128.2 | 15.39 |
| 415 | 18.19 | 1079.4 | 118.9 | 48.47 | 19.05 | 121.3 | 15.82 |
| 420 | 19.89 | 1054.0 | 132.9 | 47.15 | 19.60 | 114.5 | 16.33 |

The thermal conductivity can be calculated from Eq. (3), where the correlation for the dilute-gas function $\lambda_0(T)$ is presented by Eq. (6) and the correlation for the excess function $\Delta\lambda_R(\rho)$ is given by Eq. (7). The critical enhancement contribution $\Delta\lambda_c(\rho, T)$ is not taken into account in the present work because reliable crossover equations of state and the thermal conductivity data are still missing in the critical region. This contribution may be neglected below 373 K but not above this temperature. The correlation for the thermal conductivity is valid at temperatues from 253 to 373 K, pressures up to 30 MPa, and densities up to 1623 $kg \cdot m^{-3}$. The reason that the correlation is restricted to $T < 373$ K is the failure to account for the critical enhancement.

The viscosity can be calculated from Eq. (5), where the correlation for the dilute-gas function $\eta_0(T)$ is presented by Eq. (8), the correlation for $\eta_1(T)$ is presented by Eq. (9), and the correlation for the excess function $\Delta\lambda_R(\rho)$ is given by Eq. (10). The correlation of the viscosity is valid at temperatures from 253 to 423 K, pressures up to 20 MPa, and densities up to 1608 $kg \cdot m^{-3}$.

Table VII contains the saturation properties as a function of temperature, where a single prime and a double prime indicate values on the liquid and on the vapor side of the coexistence curve, respectively. In Tables VIII and IX the values for the thermal conductivity and the

**Table VIII.** Tabulation of the Thermal Conductivity ($mW \cdot m^{-1} \cdot K^{-1}$) of HCFC-123

| Pressure (MPa) | Temperature (K) | | | | | | | | | | | | | |
|---|---|---|---|---|---|---|---|---|---|---|---|---|---|---|
| | 260 | 270 | 273.15 | 280 | 290 | 298.15 | 300 | 310 | 320 | 330 | 340 | 350 | 360 | 370 |
| 0.1 | 87.44 | 84.70 | 83.84 | 82.00 | 79.35 | 77.22 | 76.74 | 11.04 | 11.54 | 12.03 | 12.53 | 13.02 | 13.52 | 14.01 |
| 0.5 | 87.55 | 84.81 | 83.96 | 82.12 | 79.48 | 77.36 | 76.88 | 74.32 | 71.80 | 69.30 | 66.82 | 64.35 | 14.15 | 14.62 |
| 1.0 | 87.68 | 84.95 | 84.11 | 82.28 | 79.64 | 77.53 | 77.06 | 74.51 | 72.00 | 69.52 | 67.06 | 64.61 | 62.17 | 59.70 |
| 1.5 | 87.82 | 85.10 | 84.25 | 82.43 | 79.81 | 77.70 | 77.23 | 74.70 | 72.20 | 69.74 | 67.30 | 64.88 | 62.46 | 60.02 |
| 2.0 | 87.95 | 85.24 | 84.40 | 82.58 | 79.97 | 77.87 | 77.40 | 74.88 | 72.40 | 69.95 | 67.53 | 65.13 | 62.74 | 60.34 |
| 2.5 | 88.08 | 85.38 | 84.54 | 82.73 | 80.13 | 78.04 | 77.57 | 75.07 | 72.60 | 70.17 | 67.77 | 65.39 | 63.02 | 60.65 |
| 3.0 | 88.22 | 85.52 | 84.68 | 82.88 | 80.29 | 78.21 | 77.74 | 75.25 | 72.79 | 70.38 | 67.99 | 65.64 | 63.29 | 60.95 |
| 3.5 | 88.35 | 85.66 | 84.83 | 83.03 | 80.45 | 78.38 | 77.91 | 75.43 | 72.99 | 70.59 | 68.22 | 65.88 | 63.56 | 61.25 |
| 4.0 | 88.48 | 85.80 | 84.97 | 83.18 | 80.60 | 78.54 | 78.08 | 75.61 | 73.18 | 70.79 | 68.44 | 66.12 | 63.82 | 61.54 |
| 4.5 | 88.61 | 85.94 | 85.11 | 83.32 | 80.76 | 78.71 | 78.25 | 75.79 | 73.37 | 71.00 | 68.66 | 66.36 | 64.08 | 61.82 |
| 5.0 | 88.74 | 86.08 | 85.25 | 83.47 | 80.91 | 78.87 | 78.41 | 75.96 | 73.56 | 71.20 | 68.88 | 66.60 | 64.34 | 62.10 |
| 5.5 | 88.87 | 86.22 | 85.39 | 83.62 | 81.07 | 79.03 | 78.58 | 76.14 | 73.75 | 71.40 | 69.10 | 66.83 | 64.59 | 62.38 |
| 6.0 | 89.00 | 86.35 | 85.53 | 83.76 | 81.22 | 79.20 | 78.74 | 76.31 | 73.93 | 71.60 | 69.31 | 67.06 | 64.84 | 62.65 |
| 6.5 | 89.13 | 86.49 | 85.67 | 83.91 | 81.38 | 79.36 | 78.90 | 76.48 | 74.11 | 71.79 | 69.52 | 67.28 | 65.08 | 62.91 |
| 7.0 | 89.26 | 86.63 | 85.81 | 84.05 | 81.53 | 79.52 | 79.06 | 76.65 | 74.30 | 71.99 | 69.73 | 67.51 | 65.32 | 63.17 |
| 7.5 | 89.39 | 86.76 | 85.95 | 84.19 | 81.68 | 79.67 | 79.22 | 76.82 | 74.48 | 72.18 | 69.93 | 67.73 | 65.56 | 63.43 |

| | | | | | | | | | | | | | | |
|---|---|---|---|---|---|---|---|---|---|---|---|---|---|---|
| 8.0 | 89.52 | 86.90 | 86.08 | 84.33 | 81.83 | 79.83 | 79.38 | 76.99 | 74.66 | 72.37 | 70.14 | 67.94 | 65.79 | 63.68 |
| 8.5 | 89.65 | 87.03 | 86.22 | 84.48 | 81.98 | 79.99 | 79.54 | 77.16 | 74.84 | 72.56 | 70.34 | 68.16 | 66.02 | 63.93 |
| 9.0 | 89.78 | 87.17 | 86.36 | 84.62 | 82.13 | 80.14 | 79.70 | 77.33 | 75.01 | 72.75 | 70.54 | 68.37 | 66.25 | 64.17 |
| 9.5 | 89.90 | 87.30 | 86.49 | 84.76 | 82.28 | 80.30 | 79.86 | 77.49 | 75.19 | 72.94 | 70.73 | 68.58 | 66.48 | 64.41 |
| 10.0 | 90.03 | 87.43 | 86.63 | 84.90 | 82.42 | 80.45 | 80.01 | 77.66 | 75.36 | 73.12 | 70.93 | 68.79 | 66.70 | 64.65 |
| 11.0 | 90.28 | 87.70 | 86.90 | 85.18 | 82.72 | 80.76 | 80.32 | 77.98 | 75.70 | 73.48 | 71.32 | 69.20 | 67.13 | 65.11 |
| 12.0 | 90.53 | 87.96 | 87.16 | 85.45 | 83.01 | 81.06 | 80.62 | 78.30 | 76.04 | 73.84 | 71.70 | 69.60 | 67.56 | 65.57 |
| 13.0 | 90.78 | 88.22 | 87.43 | 85.72 | 83.29 | 81.36 | 80.93 | 78.62 | 76.38 | 74.19 | 72.07 | 70.00 | 67.98 | 66.01 |
| 14.0 | 91.03 | 88.48 | 87.69 | 86.00 | 83.58 | 81.66 | 81.22 | 78.94 | 76.71 | 74.54 | 72.43 | 70.38 | 68.39 | 66.44 |
| 15.0 | 91.27 | 88.74 | 87.95 | 86.26 | 83.86 | 81.95 | 81.52 | 79.25 | 77.03 | 74.88 | 72.79 | 70.76 | 68.79 | 66.86 |
| 16.0 | 91.52 | 88.99 | 88.21 | 86.53 | 84.14 | 82.24 | 81.81 | 79.55 | 77.36 | 75.22 | 73.15 | 71.14 | 69.18 | 67.28 |
| 17.0 | 91.76 | 89.24 | 88.47 | 86.80 | 84.42 | 82.52 | 82.10 | 79.85 | 77.67 | 75.55 | 73.50 | 71.50 | 69.56 | 67.68 |
| 18.0 | 92.00 | 89.49 | 88.72 | 87.06 | 84.69 | 82.81 | 82.39 | 80.15 | 77.99 | 75.88 | 73.84 | 71.86 | 69.94 | 68.08 |
| 19.0 | 92.24 | 89.74 | 88.97 | 87.32 | 84.96 | 83.09 | 82.67 | 80.45 | 78.30 | 76.21 | 74.18 | 72.22 | 70.31 | 68.47 |
| 20.0 | 92.48 | 89.99 | 89.22 | 87.58 | 85.23 | 83.37 | 82.95 | 80.74 | 78.60 | 76.53 | 74.52 | 72.57 | 70.68 | 68.85 |
| 22.0 | 92.95 | 90.48 | 89.72 | 88.09 | 85.76 | 83.92 | 83.51 | 81.32 | 79.21 | 77.16 | 75.17 | 73.25 | 71.39 | 69.60 |
| 24.0 | 93.42 | 90.97 | 90.21 | 88.59 | 86.29 | 84.46 | 84.05 | 81.89 | 79.80 | 77.77 | 75.81 | 73.92 | 72.09 | 70.32 |
| 26.0 | 93.88 | 91.45 | 90.70 | 89.09 | 86.80 | 84.99 | 84.59 | 82.45 | 80.37 | 78.37 | 76.43 | 74.56 | 72.76 | 71.02 |
| 28.0 | 94.34 | 91.92 | 91.18 | 89.58 | 87.31 | 85.52 | 85.11 | 82.99 | 80.94 | 78.96 | 77.04 | 75.20 | 73.41 | 71.69 |
| 30.0 | 94.79 | 92.39 | 91.65 | 90.06 | 87.81 | 86.03 | 85.63 | 83.53 | 81.50 | 79.53 | 77.64 | 75.81 | 74.05 | 72.35 |

**Table IX.** Tabulation of the Viscosity ($\mu$Pa·s) of HCFC-123

| Pressure (MPa) | Temperature (K) | | | | | | | | | | | | | | | | | | |
|---|---|---|---|---|---|---|---|---|---|---|---|---|---|---|---|---|---|---|---|
| | 260 | 270 | 273.15 | 280 | 290 | 298.15 | 300 | 310 | 320 | 330 | 340 | 350 | 360 | 370 | 380 | 390 | 400 | 410 | 420 |
| 0.1 | 670.6 | 588.3 | 565.1 | 518.8 | 459.6 | 417.6 | 408.8 | 11.17 | 11.54 | 11.89 | 12.25 | 12.60 | 12.94 | 13.28 | 13.61 | 13.94 | 14.26 | 14.58 | 14.89 |
| 0.5 | 673.6 | 591.0 | 567.8 | 521.3 | 462.0 | 419.8 | 411.0 | 366.8 | 328.4 | 294.7 | 264.9 | 238.3 | 12.87 | 13.22 | 13.56 | 13.90 | 14.24 | 14.56 | 14.89 |
| 1.0 | 677.4 | 594.5 | 571.2 | 524.5 | 464.9 | 422.6 | 413.7 | 369.5 | 330.9 | 297.1 | 267.2 | 240.7 | 216.9 | 195.5 | 175.9 | 14.04 | 14.37 | 14.69 | 15.02 |
| 1.5 | 681.2 | 597.9 | 574.5 | 527.7 | 467.8 | 425.4 | 416.5 | 372.1 | 333.4 | 299.5 | 269.6 | 243.0 | 219.2 | 197.8 | 178.3 | 160.3 | 143.5 | 15.13 | 15.40 |
| 2.0 | 685.1 | 601.4 | 577.9 | 530.8 | 470.8 | 428.2 | 419.3 | 374.7 | 335.9 | 301.9 | 272.0 | 245.3 | 221.6 | 200.1 | 180.7 | 162.8 | 146.1 | 130.3 | 114.6 |
| 2.5 | 688.9 | 604.8 | 581.3 | 534.0 | 473.7 | 431.0 | 422.0 | 377.3 | 338.4 | 304.3 | 274.3 | 247.6 | 223.8 | 202.4 | 183.0 | 165.2 | 148.7 | 133.1 | 118.0 |
| 3.0 | 692.7 | 608.3 | 584.6 | 537.2 | 476.7 | 433.8 | 424.8 | 380.0 | 340.9 | 306.7 | 276.6 | 249.9 | 226.1 | 204.7 | 185.3 | 167.6 | 151.2 | 135.9 | 121.1 |
| 3.5 | 696.6 | 611.8 | 588.0 | 540.4 | 479.7 | 436.6 | 427.6 | 382.6 | 343.4 | 309.1 | 279.0 | 252.2 | 228.3 | 206.9 | 187.6 | 169.9 | 153.7 | 138.5 | 124.0 |
| 4.0 | 700.4 | 615.3 | 591.4 | 543.6 | 482.6 | 439.4 | 430.3 | 385.2 | 345.9 | 311.5 | 281.3 | 254.5 | 230.6 | 209.1 | 189.8 | 172.2 | 156.0 | 141.0 | 126.8 |
| 4.5 | 704.3 | 618.8 | 594.8 | 546.8 | 485.6 | 442.2 | 433.1 | 387.8 | 348.4 | 313.9 | 283.6 | 256.7 | 232.8 | 211.3 | 192.0 | 174.4 | 158.3 | 143.4 | 129.5 |
| 5.0 | 708.2 | 622.3 | 598.2 | 550.0 | 488.6 | 445.0 | 435.9 | 390.4 | 350.9 | 316.3 | 285.9 | 258.9 | 235.0 | 213.5 | 194.2 | 176.6 | 160.6 | 145.8 | 132.0 |
| 5.5 | 712.1 | 625.8 | 601.6 | 553.2 | 491.5 | 447.8 | 438.7 | 393.0 | 353.4 | 318.7 | 288.2 | 261.2 | 237.2 | 215.7 | 196.3 | 178.8 | 162.8 | 148.1 | 134.4 |
| 6.0 | 716.0 | 629.4 | 605.1 | 556.4 | 494.5 | 450.7 | 441.4 | 395.6 | 355.8 | 321.0 | 290.4 | 263.4 | 239.3 | 217.8 | 198.5 | 180.9 | 165.0 | 150.4 | 136.8 |
| 6.5 | 719.9 | 632.9 | 608.5 | 559.7 | 497.5 | 453.5 | 444.2 | 398.2 | 358.3 | 323.4 | 292.7 | 265.6 | 241.5 | 219.9 | 200.6 | 183.1 | 167.1 | 152.6 | 139.1 |

| | | | | | | | | | | | | | | | | | | | |
|---|---|---|---|---|---|---|---|---|---|---|---|---|---|---|---|---|---|---|---|
| 7.0 | 723.8 | 636.4 | 611.9 | 562.9 | 500.5 | 456.3 | 447.0 | 400.8 | 360.8 | 325.8 | 295.0 | 267.8 | 243.6 | 222.0 | 202.6 | 185.1 | 169.2 | 154.7 | 141.3 |
| 7.5 | 727.8 | 640.0 | 615.4 | 566.1 | 503.4 | 459.1 | 449.8 | 403.5 | 363.2 | 328.1 | 297.2 | 270.0 | 245.7 | 224.1 | 204.7 | 187.2 | 171.3 | 156.8 | 143.5 |
| 8.0 | 731.7 | 643.5 | 618.8 | 569.4 | 506.4 | 461.9 | 452.5 | 406.1 | 365.7 | 330.5 | 299.5 | 272.1 | 247.9 | 226.2 | 206.8 | 189.2 | 173.4 | 158.9 | 145.6 |
| 8.5 | 735.7 | 647.1 | 622.3 | 572.6 | 509.4 | 464.7 | 455.3 | 408.7 | 368.2 | 332.8 | 301.7 | 274.3 | 250.0 | 228.3 | 208.8 | 191.3 | 175.4 | 160.9 | 147.7 |
| 9.0 | 739.7 | 650.7 | 625.8 | 575.9 | 512.4 | 467.5 | 458.1 | 411.3 | 370.6 | 335.2 | 304.0 | 276.5 | 252.1 | 230.3 | 210.8 | 193.3 | 177.4 | 162.9 | 149.7 |
| 9.5 | 743.7 | 654.3 | 629.2 | 579.2 | 515.4 | 470.4 | 460.9 | 413.9 | 373.1 | 337.5 | 306.2 | 278.6 | 254.2 | 232.4 | 212.8 | 195.2 | 179.3 | 164.9 | 151.7 |
| 10.0 | 747.7 | 657.9 | 632.7 | 582.4 | 518.4 | 473.2 | 463.7 | 416.5 | 375.6 | 339.8 | 308.5 | 280.8 | 256.3 | 234.4 | 214.8 | 197.2 | 181.3 | 166.8 | 153.7 |
| 11.0 | 755.8 | 665.1 | 639.7 | 589.0 | 524.5 | 478.9 | 469.3 | 421.7 | 380.5 | 344.5 | 312.9 | 285.1 | 260.4 | 238.4 | 218.7 | 201.1 | 185.1 | 170.7 | 157.5 |
| 12.0 | 763.9 | 672.4 | 646.8 | 595.6 | 530.5 | 484.5 | 474.9 | 427.0 | 385.4 | 349.2 | 317.4 | 289.3 | 264.5 | 242.4 | 222.6 | 204.9 | 188.9 | 174.4 | 161.3 |
| 13.0 | 772.1 | 679.7 | 653.9 | 602.2 | 536.6 | 490.2 | 480.5 | 432.2 | 390.3 | 353.8 | 321.8 | 293.6 | 268.6 | 246.4 | 226.5 | 208.7 | 192.6 | 178.1 | 164.9 |
| 14.0 | 780.3 | 687.1 | 661.0 | 608.9 | 542.7 | 495.9 | 486.1 | 437.4 | 395.2 | 358.5 | 326.2 | 297.8 | 272.7 | 250.3 | 230.3 | 212.4 | 196.3 | 181.7 | 168.5 |
| 15.0 | 788.6 | 694.5 | 668.1 | 615.6 | 548.8 | 501.7 | 491.8 | 442.7 | 400.2 | 363.1 | 330.6 | 302.0 | 276.7 | 254.2 | 234.1 | 216.1 | 199.9 | 185.2 | 172.0 |
| 16.0 | 796.9 | 701.9 | 675.3 | 622.3 | 554.9 | 507.4 | 497.4 | 447.9 | 405.1 | 367.7 | 335.0 | 306.2 | 280.7 | 258.1 | 237.8 | 219.7 | 203.4 | 188.7 | 175.4 |
| 17.0 | 805.3 | 709.4 | 682.6 | 629.1 | 561.1 | 513.2 | 503.1 | 453.2 | 410.0 | 372.4 | 339.4 | 310.4 | 284.7 | 261.9 | 241.6 | 223.3 | 206.9 | 192.2 | 178.8 |
| 18.0 | 813.8 | 716.9 | 689.9 | 635.8 | 567.3 | 518.9 | 508.8 | 458.5 | 414.9 | 377.0 | 343.8 | 314.6 | 288.7 | 265.8 | 245.3 | 226.9 | 210.4 | 195.6 | 182.1 |
| 19.0 | 822.3 | 724.5 | 697.2 | 642.7 | 573.5 | 524.7 | 514.5 | 463.8 | 419.9 | 381.7 | 348.2 | 318.7 | 292.7 | 269.6 | 248.9 | 230.5 | 213.9 | 198.9 | 185.4 |
| 20.0 | 830.9 | 732.1 | 704.5 | 649.5 | 579.7 | 530.5 | 520.2 | 469.1 | 424.8 | 386.3 | 352.6 | 322.9 | 296.7 | 273.4 | 252.6 | 234.0 | 217.3 | 202.3 | 188.7 |

viscosity are given as a function of temperature and pressure. The values of the thermal conductivity and the viscosity in Tables VII to IX were generated directly from the representation given here with the aid of the equation of state by Younglove and McLinden [3]. The temperature and pressure ranges in which the correlations are valid can be deduced from the limits of the data tables. Any extrapolation to higher temperatures and pressures can lead to a rapid reduction in the accuracy of the predicted values and is not recommended. Because of the inconsistencies in the data sets used, the overall uncertainties of the present correlations cannot be better than $\pm 5\%$ for both properties of the background terms.

## 9. CONCLUSION

The thermal conductivity and the viscosity data of HCFC-123 have been analyzed and critically evaluated on the basis of a comprehensive literature survey. Based on the most reliable experimental data selected the residual concept correlation has been carried out.

For both properties the existing data are still scarce and somewhat contradictory except for the compressed liquid region. Experimental data are more abundant in the compressed liquid phase than in the vapor phase and lacking, in particular, in the critical and supercritical regions because the critical temperature of HCFC-123 $T_c = 456.831$ K is so high. This situation is quite different from that of HFC-134a [4]. It is not suitable for the residual concept correlation since this method is essentially more valid in the dilute-gas and dense fluid regions.

For the thermal conductivity, scattering of data and systematic deviations between different data sets are evident in the vapor phase. Experimental data are still lacking in the intermediate-density region as well as in the critical and supercritical regions. No theoretically based evaluation was feasible in the critical region because reliable crossover equations of state are still missing.

In the case of viscosity, only two sets of experimental data are available in the superheated vapor region. Systematic deviations are found between them at high temperatures and high pressures, although both measurements were performed by similar oscillating-disk viscometers in an almost same experimental condition. More precise measurements are needed for the viscosity in both gas and liquid phases.

It is believed that the final representations of the thermal conductivity and viscosity of HCFC-123 developed in this work are the most probable ones that can be produced from the available data. However, it should be noted that in the vapor phase both the thermal conductivity and the viscosity data available differed significantly among researchers. According

to the recent acceleration of the HCFC regulation, the main interest of the researchers seems to have moved from HCFCs to HFCs and their mixtures. However, more precise measurements of HCFC-123 are still needed in almost the entire fluid region to establish the reference values of transport properties. It is hoped that the present data analysis will encourage new measurements of the transport properties of HCFC-123.

## APPENDIX I

The density of HCFC-123 was calculated from the preliminary version of the Younglove and McLinden equation of state [3]. In the preliminary version the critical temperature, pressure, and density were chosen as follows:

$$T_c = 456.831 \text{ K (ITS-90)}$$

$$P_c = 3.668 \text{ MPa}$$

$$\rho_c = 550 \text{ kg} \cdot \text{m}^{-3} = 3.596417 \text{ mol} \cdot \text{dm}^{-3}$$

$$R = 8.314471 \text{ J} \cdot \text{K}^{-1} \cdot \text{mol}^{-1} \text{ (gas constant)}$$

The modified BWR equation represents the pressure $P$ as a function of the absolute temperature $T$ and the molar density $\rho$. The functional form is given as

$$P = \sum_{n=1}^{9} a_n \rho^n + \exp(-\rho^2/\rho_c^2) \sum_{n=10}^{15} a_n \rho^{2n-17} \tag{A1}$$

where the temperature dependences of the coefficient $a_i$ are given by polynomial equations of $T$. The newest version of the Younglove and McLinden equation of state is reported in Ref. 3. In the newest version the critical parameters adopted are as follows:

$$T_c = 456.831 \text{ K}$$

$$P_c = 3.6618 \text{ MPa}$$

$$\rho_c = 550 \text{ kg} \cdot \text{m}^{-3} = 3.596417 \text{ mol dm}^{-3}$$

The functional form is identical to that mentioned above. The numerical values of the coefficients were revised. However, the difference between the density values calculated from two versions is negligible and does not affect the correlations of the transport properties of HCFC-123 in the present work.

## APPENDIX II

### Results of Temperature Dependence and Temperature–Pressure Dependence Correlations

As described in Section 2, the temperature dependence and temperature–pressure dependence correlations were carried out for each physical state indenpendently to compare the existing experimental data each other. The correlations were made based on the primary data adopted in the residual concept correlation with the aid of additional secondary data to extend the valid ranges of temperature and pressure. The results of the correlations are given here for practical use. These correlations are by-products of the present work. They are not used to generate the recommended values in Tables VII–IX.

*Thermal Conductivity*

*Saturated Liquid.*

$$\lambda_{LS}(T) = 1.573143 \times 10^2 - 2.702398 \times 10^{-1} T \tag{A2}$$

where $\lambda$ is in $mW \cdot m^{-1} \cdot K^{-1}$, and $193 \leqslant T \leqslant 354$ K, with a mean deviation of 0.64%, a maximum deviation of 3.70%, and an uncertainty of 2%. This equation agrees with the recommended values in Table VII, with a mean deviation of 1.38%.

*Compressed Liquid.*

$$\begin{aligned} \lambda_{LP}(T, P) &= c_{00} + c_{01} T + (c_{10} + c_{11} T + c_{12} T^2)(P - P_s) \\ &\quad + (c_{20} + c_{21} T + c_{22} T^2)(P - P_s)^2 \end{aligned} \tag{A3}$$

$$c_{00} = 1.573143 \times 10^2, \qquad c_{01} = -2.702398 \times 10^{-1}$$

$$c_{10} = -1.155152 \times 10^{-2}, \qquad c_{11} = 1.757536 \times 10^{-3},$$

$$c_{12} = -1.274647 \times 10^{-6}$$

$$c_{20} = -6.657314 \times 10^{-3}, \qquad c_{21} = 2.383249 \times 10^{-5},$$

$$c_{22} = -2.008162 \times 10^{-8}$$

where $\lambda$ is in $mW \cdot m^{-1} \cdot K^{-1}$, $193 \leqslant T \leqslant 373$ K, $P_s \leqslant P \leqslant 30$ MPa, and $P_s$ is vapor pressure calculated by Eq. (1), with a mean deviation of 0.96%, a maximum deviation of 4.06%, and an uncertainty of 3%. This equation agrees with the recommended values in Table VIII, with a mean deviation of 1.20%.

*Vapor at Atmospheric Pressure.* See Eq. (6) in Section 5.1.1.

*Saturated Vapor.*

$$\lambda_{GS}(T) = -2.555637 \times 10^2 + 2.190260T - 6.092891 \times 10^{-3}T^2 + 5.807255 \times 10^{-6}T^3 \quad \text{(A4)}$$

where $\lambda_{GS}$ is in $mW \cdot m^{-1} \cdot K^{-1}$, and $305 \leqslant T \leqslant 443$ K, with a mean deviation of 0.88%, a maximum deviation of 1.47%, and an uncertainty of 4%. This equation represents the recommended values in Table VII, with a mean deviation of 0.97%.

*Superheated Vapor.* Correlation could not be carried out due to the serious inconsistencies of existing data.

*Viscosity*

*Saturated Liquid.*

$$\ln \eta_{LS}(T) = -4.724035 + 1.609689 \times 10^3/T + 2.913943 \times 10^{-2}T - 3.730496 \times 10^{-5}T^2 \quad \text{(A5)}$$

where $\eta_{LS}$ is in $\mu Pa \cdot s$, and $170 \leqslant T \leqslant 353$ K, with a mean deviation of 0.98%, a maximum deviation of 4.21%, and an uncertainty of 3%. This equation represents the recommended values in Table VII, with a mean deviation of 1.60%.

*Compressed Liquid.*

$$\ln \eta_{LP}(T, P) = c_{00} + c_{01}/T + c_{02}T + c_{03}T^2 + (c_{10} + c_{11}T + c_{12}T^2)(P - P_s) + (c_{20} + c_{21}/T + c_{22}T^2)(P - P_s)^2 \quad \text{(A6)}$$

$$c_{00} = -4.724035, \qquad c_{01} = 1.609689 \times 10^3$$

$$c_{02} = 2.913943 \times 10^{-2}, \qquad c_{03} = -3.730496 \times 10^{-5}$$

$$c_{10} = 1.259303 \times 10^{-1}, \qquad c_{11} = -8.473356 \times 10^{-4}$$

$$c_{12} = 1.543268 \times 10^{-6}$$

$$c_{20} = 4.207495 \times 10^{-3}, \qquad c_{21} = -7.708875 \times 10^{-1}$$

$$c_{22} = -1.818444 \times 10^{-8}$$

where $\eta_{LP}$ is in $\mu Pa \cdot s$, $233 \leqslant T \leqslant 323$ K, $P_s \leqslant P \leqslant 20$ MPa, and $P_s$ is vapor pressure calculated by Eq. (1), with a mean deviation of 1.29%, a maxi-

mum deviation of 5.17%, and an uncertainty of 4%. This equation agrees with the recommended values in Table IX with a mean deviation of 1.55%.

*Vapor at Atmospheric Pressure.* See Eq. (8) in Section 5.2.1.

*Saturated Vapor.* Experimental data could not be found in the literature.

*Superheated Vapor.*

$$\eta_{GP}(T, P) = c_{00} + c_{01}T + c_{02}T^2 + (c_{10} + c_{11}T + c_{12}T^2)(P - P_1) + (c_{20} + c_{21}T + c_{22}T^2)(P - P_1)^2 \quad \text{(A7)}$$

$$c_{00} = -2.273638, \qquad c_{01} = 5.099859 \times 10^{-2},$$

$$c_{02} = -2.402786 \times 10^{-5}$$

$$c_{10} = -2.513182, \qquad c_{11} = 1.022390 \times 10^{-2},$$

$$c_{12} = -1.150218 \times 10^{-5}$$

$$c_{20} = -9.990764, \qquad c_{21} = 4.934150 \times 10^{-2},$$

$$c_{22} = -5.833791 \times 10^{-5}$$

where $\eta$ is in $\mu$Pa · s, $323 \leqslant T \leqslant 423$ K, $0 \leqslant P \leqslant P_s$, and $P_1 = 0.101325$ MPa, with a mean deviation of 0.18%, a maximum deviation of 0.86%, and an uncertainty of 3%. This equation represents the recommended values in Table IX with a mean deviation of 0.36%.

## ACKNOWLEDGMENTS

The authors wish to express their sincere gratitude to Dr. J. E. S. Venart and Dr. W. K. Snelson for providing us with the thermal conductivity, thermal diffusivity, and viscosity data of HCFC-123 prior to publication. They are indebted to Miss K. Hamaoka for her elaborate assistance throughout the course of this work.

## REFERENCES

1. M. O. McLinden and L. Vamling, *Heat Pumps for Energy Efficiency and Environmental Progress*, J. Bosma, ed. (Elsevier Science, Amsterdam, 1993), pp. 115–126.
2. R. Tillner-Roth and H. D. Baehr, *J. Phys. Chem. Ref. Data* 1995 (in press).
3. B. A. Younglove and M. O. McLinden, *J. Phys. Chem. Ref. Data* 1995 (in press).
4. R. Krauss, J. Luettmer-Strathmann, J. V. Sengers, and K. Stephan, *Int. J. Thermophys.* **14**:951 (1993).

5. Japanese Association of Refrigeration and Japan Flon Gas Association (ed.), *Thermophysical Properties of Environmentally Acceptable Fluorocarbons-HFC-134a and HCFC-123* (Japan Association of Refrigeration, Tokyo, Japan, 1991).
6. A. Laesecke, *Viskosität und Wärmeleitfähigkeit als Thermodynamische Zustandsgrössen und ihre Darstellung durch Zustandsgleichungen*, Fortschr.-Ber. VDI, Reihe 3, Nr. 117, VDI-Verlag, Düsseldorf (1986).
7. K. Stephan, R. Krauss, and A. Laesecke, *J. Phys. Chem. Ref. Data* **16**:993 (1987).
8. V. Vesovic, W. A. Wakeham, G. A. Olchowy, J. V. Sengers, J. T. R. Watson, and J. Millat, *J. Phys. Chem. Ref. Data* **19**:763 (1990).
9. A. Laesecke, R. Krauss, K. Stephan, and W. Wagner, *J. Phys. Chem. Ref. Data* **19**:1089 (1990).
10. S. Hendl, J. Millat, E. Vogel, V. Vesovic, W. A. Wakeham, J. Luettmer-Strathmann, J. V. Sengers, and M. J. Assael, *Int. J. Thermophys.* **15**:1 (1994).
11. V. Vesovic, W. A. Wakeham, J. Luettmer-Strathmann, J. V. Sengers, J. Millat, E. Vogel, and M. J. Assael, *Int. J. Thermophys.* **15**:33 (1994).
12. Y. Tanaka, A. Miyake, H. Kashiwagi, and T. Makita, *Int. J. Thermophys.* **9**:465 (1988).
13. Y. Kobayashi, H. Ashiki, Y. Nagasaka, and A. Nagashima, *Proc. 26th Natl. Heat Transfer Symp. Japan* **1**:61 (1989).
14. J. Yata, C. Kawashima, M. Hori, and T. Minamiyama, *Proc. 2nd Asian Thermophys. Prop. Conf.* (1989), pp. 201–205.
15. M. Fukushima and N. Watanabe, *Preprint 54th Annu. Meet. Japan Soc. Chem. Eng.* (1989), p. 210.
16. J. Yata, Kyoto Institute of Technology, Kyoto, Japan, private communication (1990).
17. U. Gross, Y. W. Song, J. Kallweit, and E. Hahne, *Proc. Meet. Comm. B1 IIF/IIR*, Herzlia, Israel, (1990), p. 103.
18. I. R. Shankland, *Proc. AICh E Spring Natl. Meet. Symp. Global Climate Change Refrig. Prop.*, Orlando, FL, Mar. 18–22 (1990).
19. Y. Kobayashi, Y. Ueno, Y. Nagasaka, and A. Nagashima, *Proc. 12th Eur. Conf. Thermophys. Prop.*, Vienna, Austria, Sept. 24–28 (1990).
20. Y. Ueno, M. Sekikawa, Y. Nagasaka, and A. Nagashima, *Proc. 11th Japan Symp. Thermophys. Prop.* (1990), pp. 123–126.
21. Y. Ueno, Y, Kobayashi, Y. Nagasaka, and A. Nagashima, *Trans. Jpn. Soc. Mech. Eng.* **B57**:3169 (1991).
22. U. Gross, Y. W. Song, and E. Hahne, *Int. J. Thermophys.* **13**:957 (1992).
23. M. J. Assael and E. Karagiannidis, *Int. J. Thermophys.* **14**:183 (1993).
24. J. E. S. Venart, Fire Science Centre and Mechanical Engineering Department, University of New Brunswick, Fredericton, NB, Canada, private communication (1993).
25. O. B. Tsvetkov, Yu. A. Laptev, and A. G. Asambaev, *Int. J. Thermophys.* **15**:203 (1994).
26. R. G. Richard and I. R. Shankland, *Int. J. Thermophys.* **10**:673 (1989).
27. Y. Tanaka, S. Matsuo, C. Takata, and R. Yamamoto, *Proc. China-Japan Chem. Eng. Conf.*, Tianjin, China, Oct. (1991), pp. 80–87.
28. Y. Ueno, Y. Nagasaka, and A. Nagashima, *Proc. 12th Japan Symp. Thermophys. Prop.* (1991), pp. 225–228.
29. R. Yamamoto, S. Matsuo, and Y. Tanaka, *Int. J. Thermophys.* **14**:79 (1993).
30. K. Ohta, *M. S. thesis, Kobe University*, Kobe, Japan (1988).
31. A. Kumagai and S. Takahashi, *Int. J. Thermophys.* **12**:105 (1991).
32. D. E. Diller, A. S. Aragon, and A. Laesecke, *Proc. ASME 11th Symp. Thermophys. Prop.*, Boulder, CO, June 23–27 (1991).
33. D. E. Diller, A. S. Aragon, and A. Laesecke, *Fluid Phase Equil.* **88**:251 (1993).

34. T. Okubo and A. Nagashima, *Proc. 11th Symp. Thermophys. Prop.*, Boulder, CO, June 23–27 (1991).
35. T. Okubo and A. Nagashima, *Int. J. Thermophys.* **13**:401 (1992).
36. K. D. Peckover, S. Lagasse, and W. K. Snelson, National Research Council Canada, Ottawa, Ontario, K1A OR6 Canada, private communication (1993).
37. M. Takahashi, C. Yokoyama, and S. Takahashi, *Proc. 11th Japan Symp. Thermophys. Prop.* (1990), pp. 115–118.
38. H. Nabizadeh and F. Mayinger, *Proc. 12th Eur. Conf. Thermophys. Prop.*, Vienna, Austria, Sept. 24–28 (1990).
39. H. Nabizadeh and F. Mayinger, *High Temp.-High Press.* **24**:221 (1992).
40. M. Takahashi, C. Yokoyama, and S. Takahashi, *J. Chem. Eng. Data* **32**:98 (1987).
41. J. O. Hirschfelder, C. F. Curtiss, and R. B. Bird, *Molecular Theory of Gases and Liquids* (John Wiley & Sons, New York, 1967), Chap. 8.
42. J. Kestin, S. T. Ro, and W. A. Wakeham, *Physica* **58**:165 (1972).
43. G. H. Wang, J. E. S. Venart, and R. C. Prasad, *Proc. 3rd Asian Thermophys. Prop. Conf.*, Beijing, China, (1992), pp. 399–405.
44. J. V. Sengers, *Int. J. Thermophys.* **6**:203 (1985).
45. G. A. Olchowy and J. V. Sengers, *Phys. Rev. Lett.* **61**:15 (1988).
46. G. A. Olchowy and J. V. Sengers, *Int. J. Thermophys.* **10**:417 (1989).
47. M. Ibreighith, M. Fiebig, A. Leipertz, and G. Wu, *Fluid Phase Equil.* **80**:323 (1992).